ELSEVIER

Calculating Change Curves for Multitemporal Satellite Imagery: Mount St. Helens 1980–1995

Rick L. Lawrence and William J. Ripple†*

We developed and tested a method for analyzing multitemporal satellite imagery using change curves. The method is flexible and allows an analyst to extract specific change parameters from the curves depending on the research question of interest. Eight Landsat TM images of the Mount St. Helens, Washington, blast zone from 1984 to 1995 were geometrically and radiometrically corrected. They were then transformed to estimates of green vegetation cover. Unsupervised clustering was performed on the set of eight transformed images and polynomial curves were fit to the cluster means. From these fitted curves, parameters of interest were extracted and returned to GIS layers, including number of years to reach 10% cover, the greatest rate of cover increase during the study period, and time-integrated cover. Statistical analysis indicated that the curves did a good job of representing the change trajectories of unclustered pixels. We demonstrated the use of change curve analysis by analyzing the importance in the revegetation of Mount St. Helens of the different types of disturbance resulting from the volcanic eruption. The change curve analysis is useful in a variety of applications where the data are continuous, more than two dates of data are available, and the underlying question of interest relates to trends in the data. ©*Elsevier Science Inc., 1999*

* *Department of Land Resources and Environmental Sciences, Mountain Research Center, Montana State University, Bozeman*

† *Environmental Remote Sensing Applications Laboratory, Department of Forest Resources, Oregon State University, Corvallis*

Address correspondence to R. L. Lawrence, Dept. of Land Resources and Environmental Sciences, Mountain Research Ctr., P.O. Box 173490, Montana State Univ., Bozeman, MT 59717-3490. E-mail: rick@peak.mrc.montana.edu

Received 8 June 1998; revised 4 September 1998.

INTRODUCTION

The recovery of vegetation following the 1980 eruption of Mount St. Helens in southwest Washington has been one of the major ecological stories of the Pacific Northwest during the past two decades. From a 550 sq km homogeneous "moonscape" following the eruption on 18 May 1980, to a heterogeneous landscape that includes areas of lush vegetation today, the story of Mount St. Helens' recovery is unfolding in many ways. The study reported in this article presents one way of reading this story, using a series of satellite images to characterize vegetation change since 1980.

Analysis of vegetation is one of the most important uses of satellite remote sensing data (Lillesand and Kiefer, 1994; Coppin and Bauer, 1996). Although a variety of remote sensing techniques has been used to analyze vegetation change (e.g., Muchoney and Haack, 1994), much of the research has focused on year-to-year changes, rather than trends. Coppin and Bauer (1996) listed 11 general approaches for remote sensing change detection. Of these, one is based on a single date of imagery, eight on year-to-year changes, and two (composite analysis and multitemporal linear data transformation) can analyze two or more dates. Even when long time series have been used, the ecological analysis often focuses on year-to-year changes (e.g., Lambin and Strahler, 1994; Olsson, 1994; Eastman and Fulk, 1993).

Several studies examining seasonal vegetation change have used vegetation change profiles derived from three or more images to differentiate growing conditions among sites (Peterson, 1992), distinguish land cover types (Samson, 1993), and compare differences in vegetation types as well as year-to-year phenologic variability (Reed et al., 1994). In addition, reflectance trajectories of forest stands of different ages have been calculated to show change

REMOTE SENS. ENVIRON. 67:309–319 (1999)

655 Avenue of the Americas, New York, NY 10010

0034-4257/99/$–see front matter
PII S0034-4257(98)00092-3

in reflectance associated with succession (Peterson and Nilson, 1993).

Examination of the shape of vegetation change trajectories has been recognized in various natural resource fields as being important in understanding ecosystem responses. This has been true in studies of plant community responses. For example, Halpern and Franklin (1990) compared response curves in Douglas-fir forests as a function of disturbance intensity and stand history. Similarly, Armesto and Pickett (1986) compared vegetation growth curves in abandoned fields to test theories of different successional mechanisms. At Mount St. Helens, both del Moral and Bliss (1993) and Halpern et al. (1990) have used vegetation growth trajectories to compare recovery across diverse growing conditions created by the eruption. These studies have generally not quantified the difference in the shapes of vegetation growth curves, but they have recognized that vegetation growth trajectories reveal important information about ecosystem functions. For example, two ecosystems might each start a time series with 10% cover and end with 80% cover. However, if the first system traveled an asymptotic path to 80% cover and the second traveled a path of geometric increases, then the mechanisms controlling vegetation changes probably differed. Further, projected future conditions for each system might be vastly different.

Rigorous mathematical characterization of growth curves has long been central to biometric studies (Hunt, 1982). This approach has commonly been applied at both the individual plant and stand level. Applications have included complex theoretical growth functions for empirical applications (Richards, 1959), site-index curves (Heger, 1968), and many others. Empirical forest growth models used for stand growth prediction and economic modeling are generally based on empirically derived growth curves.

The objective of our research was to develop and test a method for characterizing vegetation change at Mount St. Helens since the eruption in 1980 using curves that model change in vegetation cover. The theoretical basis for this research was the same as presented in plant community and biometric studies. Thus, we assumed that 1) vegetation change trajectories vary spatially across the Mount St. Helens blast zone and 2) these patterns have ecological explanations and significance. The first assumption is tested by our application of the procedure we present for determining change curves. Although we present one example in this article of how the second assumption might be tested, the next stage of our research will test this assumption in detail when we attempt to explain observed patterns in the curves using ecological variables.

Methods

Study Area

For this study, we examined 25,400 ha of the blast zone from the 1980 eruptions of Mount St. Helens that have been allowed to recover with a minimum of human intervention. Vegetation in this area is highly variable both as to amount, ranging from 0% to 100% cover, and as to type, including grass, forb, and shrub dominated communities, as well as conifer and hardwood trees. A detailed description of the study area is provided in Lawrence and Ripple (1998).

Data Acquisition

We acquired eight dates of Landsat Thematic Mapper (TM) images of our study area (path 46, row 28): 19 July 1984; 26 August 1986; 31 August 1988; 9 September 1991; 10 August 1992; 29 August 1993; 31 July 1994; and 19 August 1995. Three GIS data layers were used for this study, including the boundary of Mount St. Helens National Volcanic Monument (the Monument) and a forest stand data layer, each provided by the Gifford Pinchot National Forest, and a layer detailing the types of disturbance resulting from the volcanic eruptions, which was manually digitized from a map prepared by the USGS (Lipman and Mullineaux, 1981).

Preprocessing

All images were registered to the 1991 scene, which we received georeferenced to a Universal Transverse Mercator (UTM) grid. For each registration, 10–30 ground control points were used, and total root mean square errors ranged from 0.278 to 0.432. Images were registered using nearest neighbor resampling to a 25 m pixel size.

Following registration, all images were radiometrically normalized to the 1995 image using the matched digital counts method described by Collins and Woodcock (1996). We located pixels from 30 invariate features, 10 in each of three cover types, water, mature forest, and bare soil. Of these 30 pixels, 18 (six for each cover type) were randomly selected to compute regression equations for normalization, in each case predicting 1995 digital numbers for each spectral band used in the study for each year of imagery. The 12 pixels not used to compute the regression equations were used for independent verification of the equations. For each independent verification pixel, on a year-by-year, band-by-band basis, the squared error between the regression equation predicted values and the actual 1995 values were compared to confirm that the regression equations improved the radiometric match with the 1995 image. Radiometric correction equations were used only when they improved the radiometric match based on the independent verification pixels.

The images for each date were subset using a single mask created from GIS layers. These layers were used to delineate portions of the Mount St. Helens blast zone that had not been replanted to trees following the eruption. In addition, large water bodies, areas of snow within the 1995 image, and areas of fog within the 1984 image were masked. Finally, the images for each year were transformed to estimates of percent green vegetation

cover (estimated cover) (Fig. 1), based on a regression formula developed with the 1995 image (Lawrence and Ripple, 1998).

Change Curve Fitting

Change curves may be linear or nonlinear in their parameters. For linear models, such as polynomials, least squares fits can be readily computed. For nonlinear models having more than one parameter, all parameters except the parameter of interest can be estimated and the parameter of interest can be computed (Richards, 1959). The study area contains over 400,000 pixels (25 m×25 m). Therefore, to fit a change curve on a pixel-by-pixel basis requires 400,000 curve fits. This was impractical for nonlinear models, where certain parameters must be estimated based on some *a priori* knowledge, and would be computationally intensive for linear models. Therefore, we needed a way to reduce the number of curves.

Unsupervised statistical clustering of the eight estimated cover images created clusters that were distinguished by the estimated cover trajectories (and, presumably, their vegetation cover change curves). The clustering occurred in an eight-dimension feature space where the axes were the years and the data were the estimated cover values. Thus, for example, pixels that had low values in all eight years clustered separately from pixels that began with low values and increased geometrically to high values. Generally, clusters were distinguishable by magnitude of estimated cover values (vegetation amount), rates of change, and change curve shape (e.g., straight line, geometric curve, asymptotic, sigmoid).

The clustering was performed using the Iterative Self-Organizing Clustering (ISOCLUSTER) routine in ARC/Grid software. The number of clusters chosen was arbitrary, but we estimated, based on knowledge of the study area and a pilot study, that 20–30 clusters would allow adequate distinction of different amounts of vegetation and likely vegetation trajectories, while providing a small enough number of clusters for practical data analysis. Other ISOCLUSTER parameters that could be set in ARC/Grid were maximum number of iterations (20 were permitted) and minimum cluster size (1000 pixels were specified).

A reasonable estimate of nonlinear parameters was not available. As a result, a linear model was used to fit change curves. For each cluster resulting from the ISOCLUSTER procedure, the cluster means for each year were transferred to an S-Plus data frame (MathSoft, 1995). The S-Plus linear regression model was used to fit a series of polynomials (first, second, and third order) to the means of each cluster, with the growing season following the eruption as the independent variable. These models were expressed as:

$$\text{first-order polynomial: } \mu=\beta_0+\beta_1 X,$$
$$\text{second-order polynomial: } \mu=\beta_0+\beta_1 X+\beta_2 X^2,$$
$$\text{third-order polynomial: } \mu=\beta_0+\beta_1 X+\beta_2 X^2+\beta_3 X^3,$$

where μ was the mean estimated cover value, β_0 was the estimated intercept, β_i (i=1–3) were estimated coefficients, and X was the growing season since the eruption (season 1 was prior to the first growing season). We assumed vegetation cover was 0% immediately following the eruption and prior to the first growing season, and assigned an estimated cover value of 0 to all pixels for season 1.

For each cluster, the addition of each polynomial term was tested using an extra-sum-of-squares F-test, and higher order terms were only included if the p-value for the added term was less than 0.05. Although other tests can be used to chose the best fitting polynomial, using the F-test is the most conservative (least likely to add terms). This is an important step to prevent overfitting the change curves, especially where there are a limited number of observations (in this case, nine observations, eight per cluster plus season 1) (Hunt, 1982).

The fitted change curves were tested to determine whether they adequately represented the original pixel values. We randomly selected 100 pixels from the study area. For the random pixels we computed and compared 1) the average estimated cover for the eight image dates prior to clustering and curve fitting and 2) the average estimated cover predicted by the fitted change curves for the same dates.

We extracted three parameters from the change curves to illustrate the utility of this change detection method. The parameters extracted included:

1. Number of years the curve took to reach an estimated cover of 10%, expressed as
$$\rho_1=\beta_0+\beta_1 X+\beta_2 X^2+\beta_3 X^3-10,$$
where ρ_1 = number of years to reach 10% estimated cover.
2. The greatest rate of estimated cover increase (maximum first derivative) during the study period, expressed as
$$\rho_2=\max[d\mu/dX]=\max[\beta_1+2\beta_2 X+3\beta_3 X^2],$$
where ρ_2 = the maximum first derivative of μ with respect to X.
3. Time-integrated estimated cover, as determined by the area under the curve (integral) during the study period, expressed as
$$\rho_3=\int(\beta_0+\beta_1 X_i+\beta_2 X_i^2+\beta_3 X_i^3),$$
where ρ_3=the integral of μ with respect to X_i (i=1–17).

To extract the parameters listed above, we entered the curve intercepts and coefficients into a spreadsheet and wrote three macros in Visual Basic to 1) solve each curve for estimated cover equal to 10 (the solution is in growing seasons after the eruption), 2) determine the maximum first derivative of each curve (in estimated

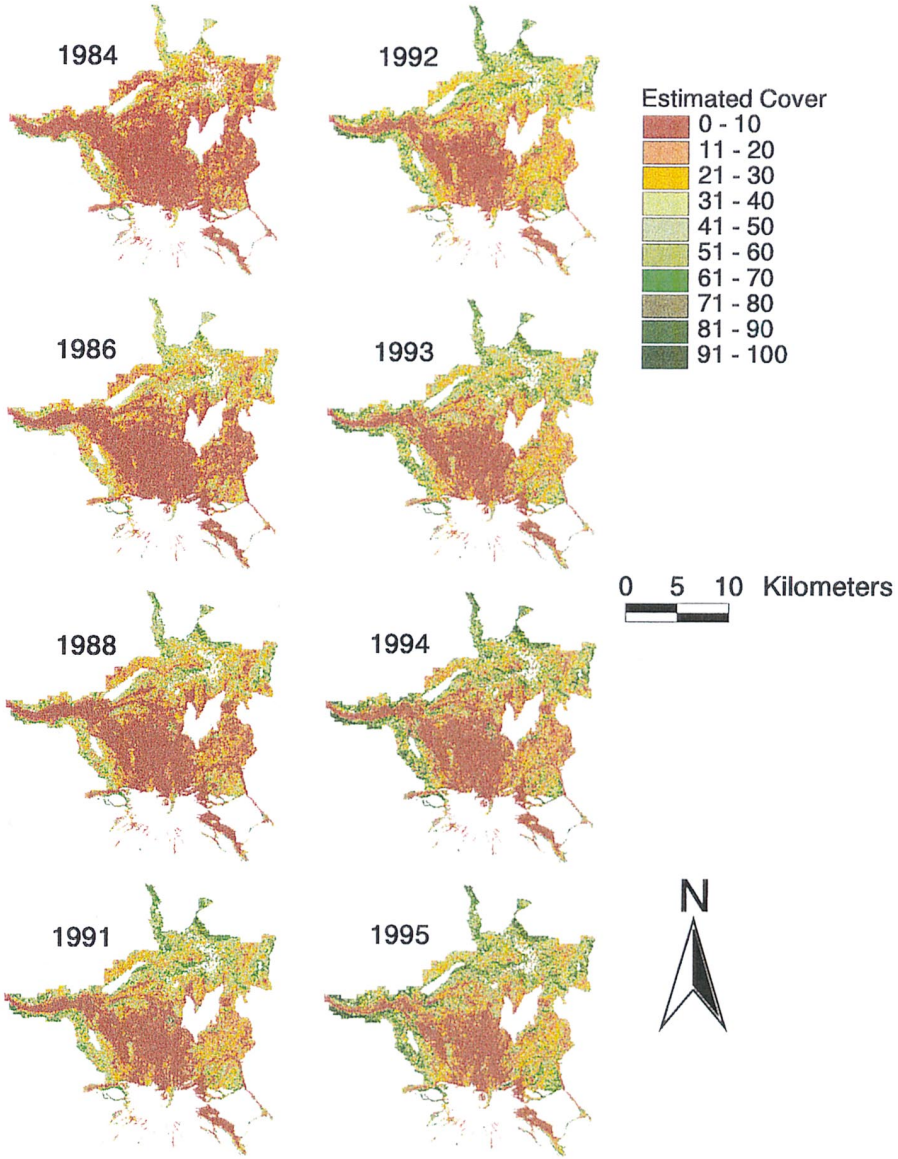

Figure 1. Spectrally estimated vegetation cover for each of the images used in the study. A regression formula was used to transform Landsat TM images to an estimate of percent green vegetation cover for each pixel.

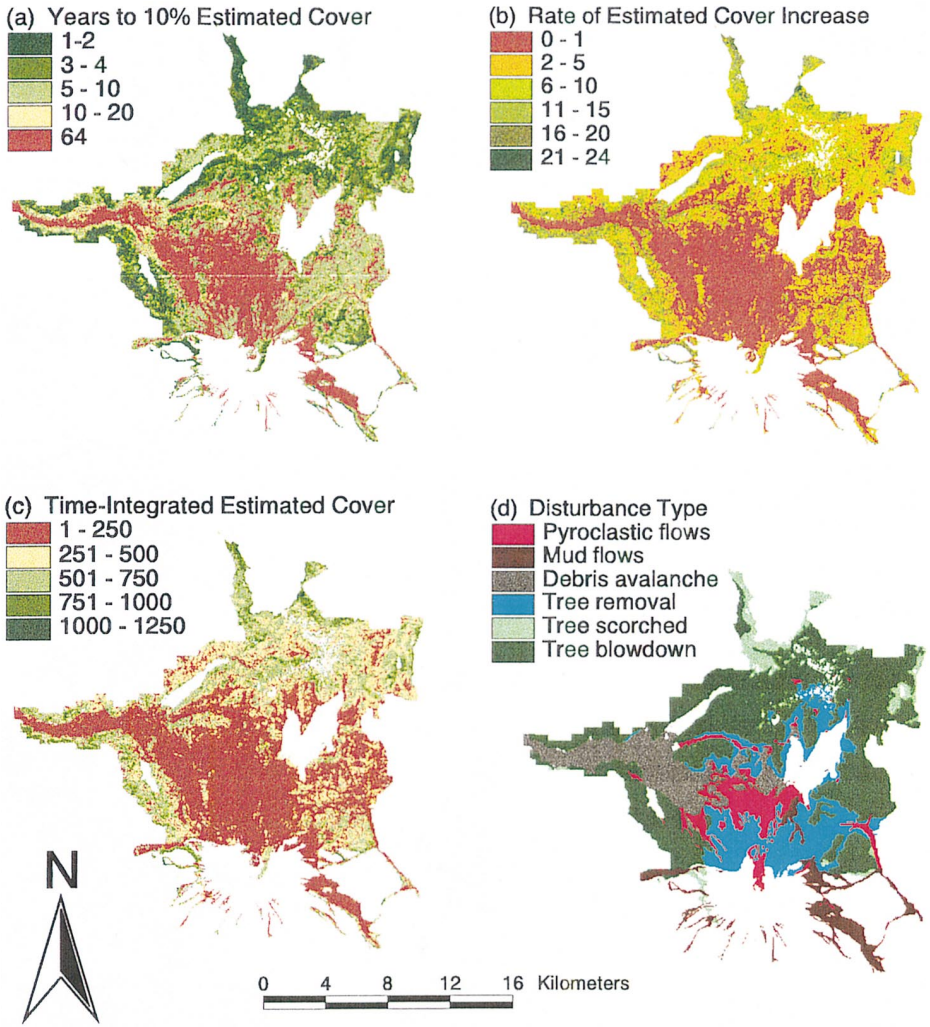

Figure 3. GIS layers used to demonstrate change curve analysis: a) Years to 10% estimated cover was obtained by solving each change curve for 10; b) rate of estimated cover increase was obtained by finding the maximum value of each change curve's first derivative during the study period; c) time-integrated estimated cover was obtained by integrating each change curve over the study period; and d) disturbance type was a categorical explanatory variable based on a map of the 1980 eruption.

cover per year), and 3) integrate the curve to determine the area under the curve (in units of integrated estimated cover, with possible values from 0 to 1600).

The results of the parameter determination were used to recode the clustered image. For example, the fitted curve for one of the clusters was:

$$\text{estimated cover} = -17.6 + 20.4\,X - 1.8\,X^2 + 0.05\,X^3,$$

where X=number of growing seasons after the eruption. A plot of this change curve is shown in column D, row 4 of Figure 2. This curve increases rapidly in early years and then becomes asymptotic. The number of growing seasons to reach 10% estimated cover was 1.5, the greatest rate of curve increase is an increase in estimated cover of 17% for each growing season, and time-integrated estimated cover was 827. Each of these values was transferred to a separate GIS layer, along with corresponding values for each of the other clusters and their associated change curves (Figs. 3a, b, and c).

Use of Change Curves

To demonstrate the utility of, and further test, the method, we applied our analysis to a specific ecological question. Previous plot-based research has noted a relationship between revegetation at Mount St. Helens and the nature of the disturbance resulting from the volcanic eruption (del Moral and Bliss, 1993; Means et al., 1982). Volcanic deposits varied greatly as to thickness and temperature (Franklin et al., 1985). The debris avalanche and mudflows were less than 100°C, the tree blowdown and scorched areas ranged from 100° to 350°C, and the pyroclastic flows were 350–850°C. The debris avalanche was 10 m to over 100 m thick, the pyroclastic flows were 1–10 m thick, deposits from mudflows and in the tree blowdown areas were about 0.1–4 m thick, and deposits in the scorched tree areas were less than 0.1 m thick.

These differences in volcanic deposits had significant effects on the presence of surviving roots and seeds, the ability of such survivors to resprout above ground, and the ability of germinating seeds to reach organic soils. We believed that these effects should be observable with our analysis. Further, we hypothesized that the nature of these effects would vary depending on how recovery was characterized. For example, we expected that the greater depth of deposits in the tree-down area, as compared to the scorched tree area, would result in slower early recovery and longer times to reach 10% cover in the tree-down area. Toward the end of our study period, however, many portions of both the tree-down and scorched areas became completely covered by vegetation. As a result, we expected less difference between in these areas for measures of ending vegetation cover or maximum rates of increase.

To test this hypothesis, from a map prepared by the USGS we created a GIS layer showing six types of volcanic disturbance, pyroclastic flows, mudflows, debris avalanche, tree removal by the directed blast, tree blowdown, and scorched trees (Fig. 3d). For 500 random points, we then extracted four measures of vegetation response (time to reach 10% estimated cover, greatest rate of estimated cover increase, time-integrated estimated cover, and 1995 estimated cover), which were each regressed against type of disturbance using linear regression, with volcanic disturbance type represented by a factor variable (which is the equivalent of an analysis of variance).

RESULTS

The clustering procedure resulted in 24 clusters representing different change trajectories (Fig. 2). (References to specific curves in this article refer to the columns and rows in Fig. 2. For example, curve D1 refers to the curve in the upper right corner of Fig. 2.) We extracted intercepts, coefficients, model p-values, and model R^2s for each of the curves (Table 1). A co-occurrence matrix for the curves and types of disturbance enabled us to describe qualitatively the spatial extent of the clusters represented by the curves with respect to the volcanic disturbances (Table 2).

With one exception (curve A1), polynomial curves fit to the cluster means explained between 84% and 100% of the variability in the cluster means. Curve A1 explained only 36% of the variability. Curve fits all had p-values$<$ 0.001, except for curve A1 which had a p-value of 0.09. However, because the curves were fit to temporal data, which are not independent, p-values might not accurately reflect the quality of the curve fits. Of the 24 fitted polynomial curves, six were first order, six were second order, and 12 were third order.

Our test of the difference between pixel-level estimates of vegetation cover and estimates of vegetation cover from the change curves estimated values for the unfitted pixels at 0.5% less than the change curve estimates, with a 95% confidence interval from −1.2% to 0.2%. We believe the 0.5% difference is ecologically insignificant. The inclusion of 0 in the confidence interval indicates that, statistically, there was no difference between the original pixels and the values estimated by the change curves. Thus, there was convincing statistical evidence that the change curves did a good job of reflecting the response of the original pixels.

The change curves graphically demonstrated that areas with similar beginning and ending values might have very different change trajectories (for example, Curves D1, C2, and D6 on Fig. 2). Specific parameters from the change curves were extracted (Table 3) and used to reclassify the clusters resulting from the multivariate clustering (Figure 3). Throughout the study area, the number of years to reach 10% estimated cover varied from slightly over 1 year to almost 11 years (one curve did not reach 10% by the end of the study period), maximum rates of

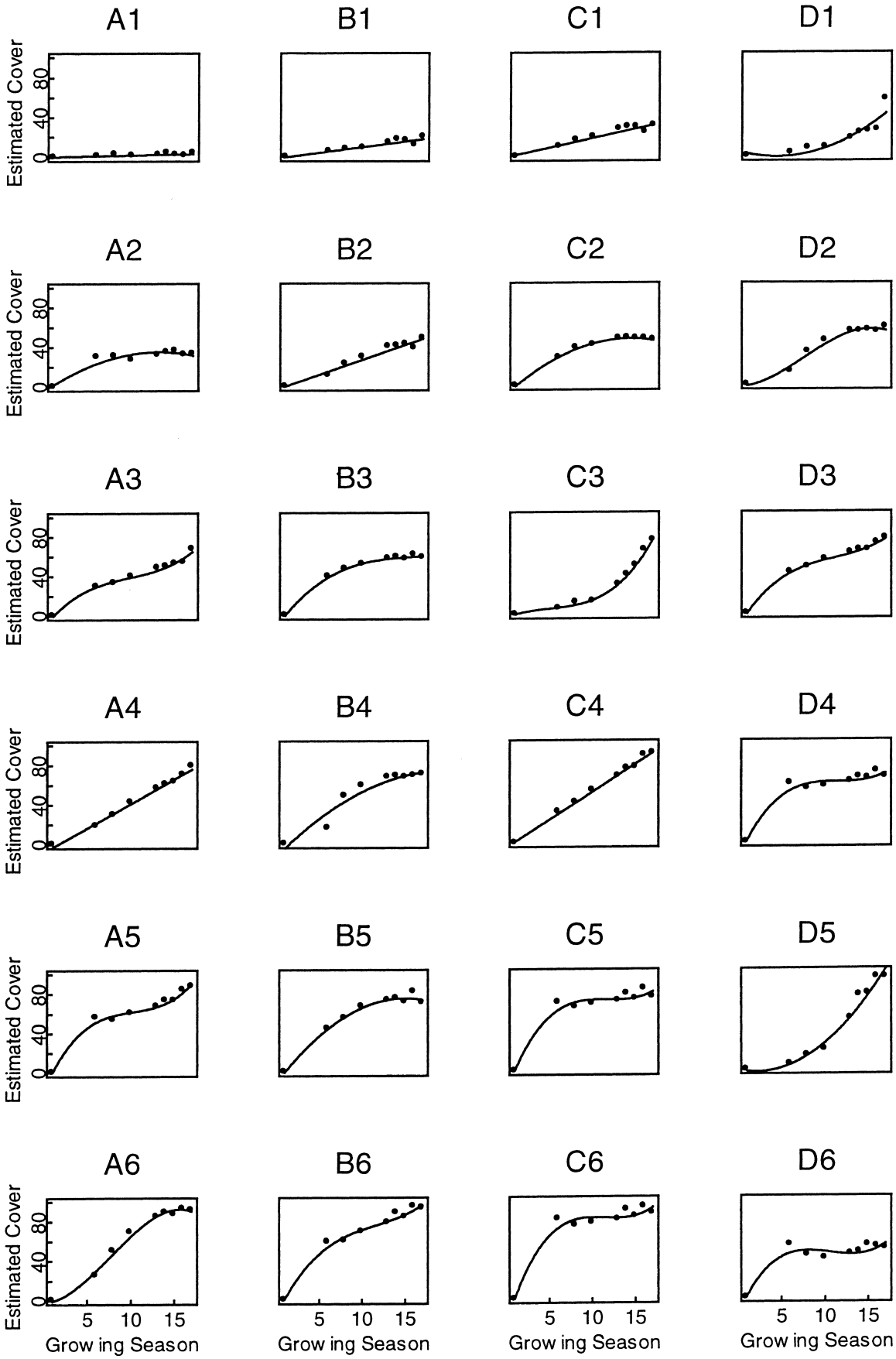

Figure 2. Change curves fitted to 24 cluster means resulting from multitemporal clustering of the eight estimated cover layers in Figure 1. The axes are the same for each graph. The *X*-axis represents the growing seasons from 1 (prior to the first growing season after the eruption) to 17 (1995). The *Y*-axis represents estimated green vegetation cover from 0% to 100%.

Table 1. Statistics for Change Curves Fitted to Means of Multitemporal Clusters[a]

Curve Designation	β_0 *(Intercept)*	β_1 *(X coefficient)*	β_2 *(X^2 coefficient)*	β_3 *(X^3 coefficient)*	R^2
A1	0.22	0.16	—	—	0.36
B1	−1.32	1.13	—	—	0.89
C1	−0.30	1.89	—	—	0.93
D1	4.65	−2.34	0.27	—	0.84
A2	−3.35	5.85	−0.22	—	0.90
B2	−2.51	3.00	—	—	0.95
C2	−7.50	7.64	−0.27	—	1.00
D2	−1.65	0.21	0.72	−0.03	0.98
A3	−10.45	11.29	−0.96	0.03	0.99
B3	−11.34	12.13	−0.73	0.02	1.00
C3	−3.01	3.51	−0.52	0.03	1.00
D3	−13.66	14.8	−1.15	0.03	1.00
A4	−7.73	4.91	—	—	0.99
B4	−13.06	8.82	−0.23	—	0.93
C4	−4.38	5.62	—	—	0.99
D4	−17.63	20.38	−1.76	0.05	0.96
A5	−18.53	20.94	−1.91	0.06	0.99
B5	−11.30	11.52	−0.38	—	0.98
C5	−21.00	24.21	−2.07	0.06	0.95
D5	0.78	−2.06	0.47	—	0.98
A6	−2.45	0.73	1.07	−0.05	0.99
B6	−16.31	18.39	−1.35	0.04	0.98
C6	−24.78	28.60	−2.52	0.07	0.96
D6	−16.79	20.14	−2.01	0.06	0.90

[a] Curve designations refer to the columns and rows of Figure 2. R^2 values indicate the percentage of variation in cluster means explained by the fitted curves.

increase from less than 0.2% to almost 24% per year, and time-integrated estimated cover from 26 to 1121. When we used these parameters as response variables, type of volcanic disturbance explained 1) 40% of variability in time to reach 10% estimated cover (p-value$<$0.0001), 2) 21% for maximum rate of estimated cover increase (p-value$<$ 0.0001), 3) 33% of variability in time-integrated estimated cover (p-value$<$0.001), and 4) 33% of variability in 1995 estimated cover (p-value$<$0.0001).

DISCUSSION

Our study showed that change curves can be an effective tool in characterizing vegetation change as mapped by digital imagery. We realized that the method we used (a combination of multivariate clustering and curve fitting) resulted in the loss of information from the original images because pixel values differed from their respective cluster means and the curve fits contained residual error. Both of these conditions can be expected in every application of this method. Our results, however, indicated that, at least for our study, this loss of information was not significant. The comparison of average estimated cover from unfitted pixel values and from curve estimates provided evidence that the curve fitting technique accurately represented the trajectories present in the original data.

We were concerned that the fit of curve A1, representing 6976 ha, had an R^2 of 0.36. Our examination of the spatial extent of the pixels represented by this curve (Table 2) explained these results. This curve represented areas that were most severely affected by the eruption and that had little vegetation response as of the end of the study period (generally less than 5% cover). The vegetation in these areas consisted largely of annuals and sparse shrubs. We believe that, because of the sparse vegetation in this area and the slow rate of increase in cover, sources of annual variability not related to trends in vegetation change were stronger relative to overall vegetation trends than in other areas. These sources of variability might have included annual variability in soil moisture, uncorrected radiometric differences, annual climatic differences resulting in phenological variability, and differences each year in length of growing seasons prior to image acquisition. The overall trend was close to flat (an increase of less than 0.2% vegetation cover per year). Thus, these variations on a year-to-year basis were not readily modeled with change curves, although the curve did represent the overall flat trend. Further, there was less variability in the data for curve A1 than the other curves. Thus, in spite of the low percentage of variability explained, the residual standard error for curve A1 was less than 22 of the other 23 curves.

The change curves (Fig. 2) can be grouped into three major types, based on disturbance types. The curves revealed much about the nature of revegetation in these

Table 2. Spatial Extent of Clusters Relative to Their Fitted Curves and the Volcanic Disturbance[a]

Curve Designation	*Area (has)*	*Spatial Extent Relative to Volcanic Disturbance*
A1	6976	Pyroclastic flows, large portions of debris avalanche, and mud flows
B1	4551	Pyroclastic flows, debris avlanche, and mud flows
C1	2809	Tree blowdown and tree removal
D1	1051	Debris avalanche and mud flows
A2	1246	Scattered locations in tree blowdown and tree removal
B2	1711	Primarily in tree blowdown
C2	983	Scattered in tree blowdown and tree scorched
D2	697	Primarily in tree blowdown
A3	493	Primarily in tree blowdown
B3	798	Scattered in tree blowdown and tree scorched
C3	432	At edges of debris avalanche and mud flows
D3	458	Scattered in tree blowdown and tree scorched
A4	298	Scattered in tree blowdown and tree scorched
B4	278	Scattered in tree blowdown and tree scorched
C4	175	Primarily in tree blowdown
D4	403	Primarily in tree scorched
A5	207	Scattered in tree blowdown and tree scorched
B5	200	Scattered in tree blowdown and tree scorched
C5	169	Scattered in tree blowdown and tree scorched
D5	139	At edges of debris avlanche
A6	97	In tree blowdown and tree scorched in Toutle River Valley
B6	149	In tree blowdown and tree scorched in Toutle River Valley
C6	110	In tree scorched and at edges of mud flows
D6	475	Scattered in tree blowdown and tree removal areas

[a] Curve designations refer to the columns and rows of Figure 2.

areas. Generally, curves A1, B1, and C1 occurred on the pyroclastic flows, debris avalanche, tree removal areas, and mud flows (Table 2). These were areas most severely affected by the eruptions. All three of these curves were represented by first order polynomials that remain at low levels of cover at the end of the study period.

Curves D1, C3 and D5 occurred primarily at the edges of mud flows and the debris avalanche (Table 2). Each of these curves was characterized by very slow increases in early years, with rapidly increasing rates of recovery toward the end of the study period. Many of these areas have had substantial establishment of alder, which took several years to establish, but is now growing rapidly.

The remaining curves were found primarily in the tree blowdown and tree-scorched areas, although they were also found to some extent in the tree removal areas. These curves were generally characterized by rapid increases in cover in early years, in many cases becoming asymptotic toward the end of the study period at approximately 50–80% estimated cover. We believe the shape of these curves reflected the effect of buried surviving vegetation and seeds that existed in much of these areas following the eruption. These survivors provided for rapid revegetation. However, factors such as substantial numbers of downed trees prevented these areas from becoming fully occupied. In addition, curves that represented a substantial amount of the tree removal area (curves A2 and D6) generally became asymptotic at lower levels of cover than curves for other areas.

The extensive field data necessary to conduct a validation of our results were not available because this study was conducted retrospectively. However, we were able to compare qualitatively some of our results with previously published trajectories from plot based studies at Mount St. Helens. Trajectories of percent mean cover from 1980 to 1990 have been published for plots in the scour, lahar, blast, Pumice Plains, and Plains of Abraham areas (del Moral and Bliss, 1993). The mudflow scour areas were primarily associated with our curve D1 (Table 2), while the other areas were primarily associated with curves A1 and B1. The plot based curves were consistent with our derived curves, with the scour area increasing to approximately 14% by 1990 in the plot based study and 15.5% in our study, and the other areas increasing very slowly to no more than 4% by 1990 in the plot based study and 2.1% in our study.

Similar trajectories have been published for 1980–1986 with respect to tree blowdown and tree-scorched areas (Halpern et al., 1990). By 1986, both blowdown and scorched plots had between 10% and 15% cover. On a landscape scale, these areas have been noted to contain significant variability (Franklin et al., 1988). This is supported by our study, where 15 different change curves are associated with these areas (Table 2). Although many of our curves associated with these areas predicted greater vegetation cover than that shown in the plot-based studies, the plot-based results are within the range of our predicted values for blowdown and scorched areas.

The utility of this approach for change detection was

Table 3. Parameters Extracted from Change Curves

Curve Designation[a]	*Years to Reach 10% Estimated Cover*[b]	*Time-Integrated Estimated Cover*[c]	*Greatest Rate of Estimated Cover Increase*[d]
A1	64.0	26	0.2
B1	10.1	141	1.1
C1	5.5	265	1.9
D1	10.5	177	6.8
A2	2.5	422	5.4
B2	4.2	383	3.0
C2	2.5	542	7.1
D2	4.3	520	5.7
A3	2.2	568	9.5
B3	1.9	692	10.7
C3	8.2	326	15.9
D3	1.8	749	12.6
A4	3.6	579	4.9
B4	2.8	689	8.4
C4	2.5	735	5.6
D4	1.5	827	17.0
A5	1.5	881	17.3
B5	1.9	845	10.8
C5	1.4	982	20.2
D5	7.1	486	14.0
A6	3.3	839	8.9
B6	1.6	980	15.8
C6	1.3	1121	23.8
D6	1.5	658	16.3

[a] Curve designations refer to columns and rows of Figure 2.
[b] Obtained by solving the curve for 10.
[c] Obtained by integrating the curve over the study period.
[d] Obtained by finding the maximum value of the curve's first derivative during the study period.

demonstrated by our volcanic disturbance type analysis. As we expected, based on previous plot-level studies, vegetation recovery was significantly correlated to type of volcanic disturbance (all p-values<0.001). There were, of course, many other factors that affected vegetation recovery as well. This resulted in a substantial percentage of unexplained variance in our analysis.

Although the significance of disturbance type could have been shown through other analyses, our change curve analysis permitted us to make additional distinctions. While we expected that disturbance type would significantly affect revegetation throughout the study period, it was important to understand why the amount of variance explained varied with the measure of vegetation recovery used.

The largest amount of variation explained (40%) was with respect to number of years to reach 10% estimated cover. This was a measure of early vegetation response. Previous studies noted the importance of surviving seeds and below-ground portions of sprouting species in the early response at Mount St. Helens (Franklin et al., 1985). We expected the presence of survivors would vary significantly with the type of disturbance and be reflected in the number of years to reach 10% cover. For example, in the tree-scorched zone, above-ground vegetation was killed, but substantial below-ground vegetation should have survived beneath a relatively thin layer of fresh volcanic deposit. However, in the tree blowdown zone, the disturbance was more severe and deposits averaged somewhat thicker. In the debris avalanche and pyroclastic flow areas, deposits were too thick for spouting vegetation to penetrate, even if survivors existed. Compared to the debris avalanche, in the mud flows there was greater opportunity for uprooted plants to be deposited on or near the surface where they might resprout. These different mechanisms related to disturbance type strongly influenced early vegetation recovery and, as a result, disturbance type explained a large amount of variance in number of years to reach 10% cover.

Although statistically significant, type of disturbance only explained 33% of the variance in 1995 estimated cover. We believe this occurred because other factors had increasing influence over revegetation with time. For example, in substantial portions of both the tree scorched and tree blowdown zones, estimated cover had become asymptotic by 1995 (Table 1, Fig. 2). Thus, these areas became less distinguishable by disturbance type. Portions of the debris avalanche (especially those represented by curve D1), which in many cases did not reach 10% estimated cover for over 10 years, have now rapidly increased to 40% estimated cover or more, decreasing their distinction from portions of the tree blowdown

zone. We believe that, in general, while the volcanic disturbance mechanisms dominated early recovery, over time other factors have played an increasing role in the variability of patterns across the Mount St. Helens landscape. These factors include an increasing influence of stochastic factors, such as seed dispersal mechanisms and weather influences.

Type of disturbance explained the least amount of variance (21%) with respect to greatest rate of estimated cover increase. We believe that this variable responded to a more complex array of influences. The debris avalanche along the Toutle River Valley was an example. The central portion of this area had a very slow rate of recovery throughout the study period, possibly as a result of the continued scouring effect of the Toutle River in the active river channel that runs through this area. On the other hand, the edges of this area, after slow initial recovery, have experienced some of the greatest rates of increase in cover throughout the entire study area with the establishment and growth of alder. The pattern of recovery along the edges of the debris flow, with vegetation progressing from the edges, indicates that this increased rate of recovery might be related to proximity to seed sources and differences in substrates within the debris flow. In addition, for many curves the maximum rate of increase occurred at the end of the study period, indicating that true maximum rates of increase might not be reflected during the study period. Thus, factors other than type of disturbance might explain more of the variability in maximum rate of increase than in other variables.

CONCLUSIONS

Our approach demonstrated the advantages of using computed curves for change analysis. Inherent in the change curves were various parameters relating to the trends in cover changes over time. The particular parameter of interest for a particular hypothesis can be computed from the curve and returned to a GIS layer for spatial analysis. These parameters can be found by solving the curve for a particular level of the response variable (e.g., when did vegetation cover reach a certain level or when was maximum vegetation cover reached), a particular time (e.g., what was the estimated cover percentage at a particular year or what was the maximum cover reached), or other properties of the curve (integral, maximum first derivative, or order of the polynomial).

We believe that our approach will be most useful when the question of interest relates to pixel level trends, as opposed to categorical changes. For our study in disturbance recovery, this involved changes in green vegetation cover over time. In addition to disturbance ecology, other areas of study that we believe would benefit from this approach include 1) growth rates of forest stands, such as increases in biomass in managed forests, 2) successional processes, such as changes from deciduous forests to mixed stands to conifer, 3) seasonal changes associated with plant phenology, or 4) rates of urbanization, such as changes at the pixel level in percent of land converted from agriculture to urban, but not categorical changes in pixels from agricultural to urban. Thus, this technique is applicable to sets of continuous data (not thematic), with more than two dates, where the question of interest relates primarily to trends.

The authors wish to acknowledge the assistance of Warren Cohen, U.S. Forest Service Pacific Northwest Research Station, Doretta Collins, Washington State Department of Natural Resources, Thomas Erkert, Gifford Pinchot National Forest, and Peter Frenzen and Gordon Glockner, Mount St. Helens National Volcanic Monument, for their support in this project. Frederick Swanson, U.S. Forest Service Pacific Northwest Research Station, Janet Franklin, San Diego State University, and Peter Frenzen provided constructive reviews of a draft of this article. Partial funding for this project was provided through the National Science Foundation (Grant #GER-9452810) under the auspices of the NSF Graduate Research Fellowship in Landscape Studies.

REFERENCES

Armesto, J. J., and Pickett, S. T. A. (1986), Removal experiments to test mechanisms of plant succession in oldfields. *Vegetatio* 66:85–93.

Collins, J. B., and Woodcock, C. E. (1996), An assessment of several linear change detection techniques for mapping forest mortality using multitemporal Landsat TM data. *Remote Sens. Environ.* 56:66–77.

Coppin, P. R., and Bauer, M. E. (1996), Digital change detection in forest ecosystems with remote sensing imagery. *Remote Sens. Rev.* 13:207–234.

del Moral, R., and Bliss, L. C. (1993), Mechanisms of primary succession: insights resulting from the eruption of Mount St. Helens, In *Advances in Ecological Research* (M. Began and A. Fitter, Eds.), Academic, London, Vol. 24, pp. 1–66.

Eastman, J. R., and Fulk, M. (1993), Long sequence time series evaluation using standardized principal components. *Photogramm. Eng. Remote Sens.* 59:1307–1312.

Franklin, J. F., Frenzen, P. M., and Swanson, F. J. (1988), Recreation of ecosystems at Mount St, Helens—contrasts in artificial and natural approaches. In *Rehabilitating Damaged Ecosystems* (J. Cairns, Jr., Ed.), CRC Press, Boca Raton, FL, pp. 1–37.

Franklin, J. F., MacMahon, J. A., Swanson, F. J., and Sedell, J. R. (1985), Ecosystem responses to the eruption of Mount St. Helens. *Natl. Geogr. Res.* 1:198–216.

Halpern, C. B., and Franklin, J. F. (1990), Physiognomic development of *Pseudotsuga* forests in relation to initial structure and disturbance intensity. *J. Veg. Sci.* 1:475–482.

Halpern, C. B., Frenzen, P. M., Means, J. E., and Franklin, J. F. (1990), Plant succession in areas of scorched and blown-down forest after the 1980 eruption of Mount St. Helens, Washington. *J. Veg. Sci.* 1:181–194.

Heger, L. (1968), A method of constructing site-index curves from stem analyses. *For. Chronicle* 21:11–15.

Hunt, R. (1982), *Plant Growth Curves: The Functional Approach to Plant Growth Analysis*, University Park Press, Baltimore, 248 pp.

Lambin, E. F., and Strahler, A. H. (1994), Change vector analysis in multitemporal space: a tool to detect and categorize land-cover change processes using high temporal-resolution satellite data. *Remote Sens. Environ.* 48:231–244.

Lawrence, R. L., and Ripple, W. J. (1998), Comparisons among vegetation indices and bandwise regression in a highly disturbed, heterogeneous landscape: Mount St. Helens, Washington. *Remote Sens. Environ.* 64:91–102.

Lillesand, T. M., and Kiefer, R. W. (1994), *Remote Sensing and Image Interpretation*, 3rd ed., Wiley, New York, 750 pp.

Lipman. P. W., and Mullineaux, D. R., Eds. (1981), *The Eruptions of Mount St. Helens, Washington*, Geological Survey Professional Article 1250, U.S. Government Printing Office, Washington, DC, 844 pp.

MathSoft, Inc. (1995), *S-PLUS Users' Manual*, MathSoft, Inc., Seattle.

Means, J. E., McKee, W. A., Moir, W. H., and Franklin, J. F. (1982), Natural revegetation of the northeastern portion of the devastated area. In *Mount St. Helens—Five Years Later* (S. A. C. Keller, Ed.), Eastern Washington University Press, Cheney, WA, pp. 93–103.

Muchoney, D. M., and Haack, B. N. (1994), Change detection for monitoring forest defoliation. *Photogramm. Eng. Remote Sens.* 60:1243–1251.

Olsson, H. (1994), Changes in satellite-measured reflectances caused by thinning cuttings in boreal forests, *Remote Sens. Environ.* 50:221–230.

Peterson, U. (1992), Seasonal reflectance factor dynamics in boreal forest clear-cut communities. *Int. J. Remote Sens.* 13:753–772.

Peterson, U., and Nilson, T. (1993), Successional reflectance trajectories in northern temperate forests. *Int. J. Remote Sens.* 14:609–613.

Reed, B. C., Brown, J. F., VanderZee, D., Loveland, T. R., Merchant, J. W., and Ohlen, D. O. (1994), Measuring phenological variability from satellite imagery. *J. Veg. Sci.* 5:703–714.

Richards, F. J. (1959), A flexible growth function for empirical use. *J. Exp. Bot.* 10:290–300.

Samson, S. A. (1993) Two indices to characterize temporal patterns in the spectral response of vegetation. *Photogramm. Eng. Remote Sens.* 59:511–517.